BAYERO JOURNAL OF ENGINEERING AND TECHNOLOGY (BJET) VOL.16 No.2, MAY, 2021
PP 115-125 ISSN: 2449 – 0539

PARTIAL RELATIVE GAIN ARRAY SELECTION OF UPFC SIGNALS FOR DAMPING INTER-AREA OSCILLATIONS

Ibrahim Hassan[1], Nuraddeen Magaji[2], Bala Boyi Bukata[3].

[1, 2, 3] Department of Electrical Engineering, Bayero University Kano, P.M.B. 3011 Kano, Nigeria

ABSTRACT

Stabilising power system operations has been a critical phenomenon in maintaining synchronism among system's generating units. With growing power system complicities, the use of traditional damping methods like the proportional-integral-derivative (PID), and the relative gain array (GRA) can no longer meet customers' sensitive load proliferation. This paper utilises a modified partial relative gain array (PRGA) algorithm for sourcing the control signals in unified power factor controller (UPFC) to damp oscillating inter-area network. The 2-area 13-bus system is used to implement this technique, and it has proven to be more effective in determining the integral controllability with integrity (ICI) of uncertain modeling errors with increased sensitivity as compared to the traditional GRA technique. Using PRGA techniques, appropriate control signals were selected that were used to shift the critical eigenvalues of the power systems more to the left of j-ω axis, thereby damping the inter-area oscillation by increasing the damping ratio from 0.0231 to 0.13, and reducing the damping rate from 6 seconds achieved without UPFC down to 4 seconds with UPFC.

Keywords: FACTS, Inter-area-oscillations, PID, Partial relative gain array, Unified power factor controller

1. INTRODUCTION

Stabilising power system operations has been a critical phenomenon in maintaining security in the event of any reliable contingency. However, modern power systems are operated closest to their stability limits due to economic and environmental constraints, C. W. Taylor (1994). Hence, operating a stable and secure power system comes in with lots of challenges. Recently, voltage instability has particularly been considered by researchers to be the chief source of system insecurity, P. Bikash and C. Balarko (2005).

Technically, electro-mechanical oscillations are power system disturbances caused by interchanges between potential and kinetic energies which are liable for shifting the equilibrium point of the system Dhanraj C. et al., (2015). As a result, the rotor of the interconnected synchronous machine oscillates with the system's parameters like bus voltage, frequency, real and reactive powers. Therefore, to maintain system security, the stability of these oscillations must be sustained.

Conversely, inter-area oscillation is a special type of electro-mechanical oscillation where groups of loosely couple machines of large interconnected power system oscillate against each other with frequencies ranging from 0.1Hz to 0.8Hz. If left unchecked, the phenomenon can lead to system collapse. However, some supplementary control measures were proposed to enhance the system's operation and, to overcome the menace C. W. Taylor (1994). The flexible ac transmission systems (FACTS) devices are currently being deployed to seamlessly control the power flow in a transmission system by largely controlling the bus voltage magnitude, voltage angles, and the line admittance parameters, C. W. Taylor (1994), P. Bikash and C. Balarko (2005), and N. Magaji and M. W. Mustafa (2008). However, the challenge for selecting the appropriate stabilising signals for damping inter-area oscillations still remains a research element problem.

So many contributions have been advanced in the literature in search for solutions to the problem. For example,

determining the optimal locations for input signals in FACTS devices using decentralized control theory of relative gain array (RGA) was presented in, A. Kazemi and H. Andami. Other related RGA based FACTS dampers for normal power system stability analyses can be found in, P. Zhang, A. R. Messina, A. Coonick, and B. J. Cory (1998), N. Magaji and M. W. Mustafa (2009), M. M. Farsangi et al (2004), S. Skogestad and I. Postlethwaite (2005), D. Z.Chen et al (2006). However, in the case of damping inter-area oscillations, Eigen-value analysis for designing unified power flow controllers (UPFC) as well as its power frequency model for improving transient and small signal stability, were addressed in, S. A NabaviNiaki, M. Reza Iravani (2002), and C. M. Shen et al (2000), respectively. Additionally, power oscillation damping (POD) control was also used to enhance the active (P) and reactive (Q) power components within the transmission network, R. D. Saxena et al (2012).

Arzehu et al. (2018) used Bees Algorithm to optimize the parameters of FACTS-POD (Power Oscillation Damping) on the WECC 9-bus network. This has resulted in shifting the inter-area modes eigenvalues of the network more to the left of the J-ω axis, thereby damping the inter-area oscillation. However this resulted in setting time of 6 seconds which is longer than the settling time achieved by robust damping controller.

Jeffrey U., (2019) identifies a significant deficiency in the literature on the application of the relative gain array (RGA) formalism in the case of singular matrices. Specifically, it is shown that the conventional use of the Moore-Penrose pseudo-inverse is inappropriate because it fails to preserve critical properties that can be assumed in the nonsingular case. It is then shown that such properties can be rigorously preserved using an alternative generalized matrix inverse.

This paper utilises a modified partial relative gain array (PRGA) algorithm for sourcing the control signals in unified power factor controller (UPFC) to damp oscillating inter-area network. The idea is implemented in the two-area 13-bus system, and it has proven to be more effective when compared to the traditional relative gain array (GRA) method, in the sense that the traditional GRA does not guarantee stabilising a large decentralised MIMO system when it is used to select the input-output pairs of the array configuration. This is because some of the control loops may not be visible to RGA due to lack of integral controllability with integrity (ICI) in the system Jeffrey U., (2019). A system is considered ICI if its stability is not affected by commissioning or decommissioning individual controllers within. Solving this problem requires further screening of the control structures, which could be achieved by the PRGA technique.

The remainder of the paper is organized as follows: section II presents the UPFC Model. While analysis of interactions between control loops in respect with the GRA is given in section III. The methodology adapted in implementing the idea is covered under section IV. Section V presents results and discussions on the findings of this work. The paper ends in conclusion and laid down references.

2. UPFC MODEL

The unified power flow controller (UPFC) is a hybrid FACTS device. In other words, it comprises both the series and shunt power converters connected to a common capacitor, and coupling transformers with the desire to enable reactive current exchange through the point of common coupling (PCC) along the transmission line as shown in Fig. 1. The two voltage source converters (VSC1 & 2) are programmed to either absorb or inject reactive current ahead of the coupling reactance to compensate power deficiencies as the case may be. The dc capacitor is used to replenish and maintain the system's real power demand as it depletes

via the shunt converter, G. Rogers (2008).

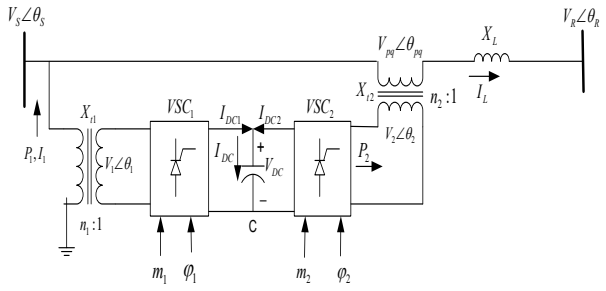

Figure 1: UPFC on a transmission line, G. Rogers (2008)

Control of the voltage magnitudes and their phase angles for both shunt and series transformers is achieved by manipulating the modulation indices m1 & m2, and the firing angles φ1 & φ2 of VCS1 and VSC2, respectively. It should be observed here that four indices (m1, m2, φ1 and φ2) are manipulated in order to control four parameters (Vac, Vdc, P, and Q). Hence, different control algorithms could be used to provide the desired feedback control loop for each of these parameters.

The UPFC model used in this research is in accordance to, C. W. Taylor (1994) and is laid down thus:

a) The dc link charging dynamics is given as;

$$I_{DC} = C\frac{dV_{DC}}{dt} \quad \cdots \quad (1)$$

$$I_{DC} = I_{DC1} + I_{DC2} \quad \cdots \quad (2)$$

b) For an ideal inverter, the active power exchange with transmission system is gives as:

$$P_1 = V_{dc}I_{dc1}/S_B \quad \cdots \quad (3)$$

$$P_2 = -V_{dc}I_{dc2}/S_B \quad \cdots \quad (4)$$

From (1), (2), (3) and (4)

$$CV_{dc}\frac{dV_{dc}}{dt} = (P_1 - P_2)S_B \quad \cdots \quad (5)$$

c) For the ac side, P1and P2 are given as:

$$P_1 = \mathrm{Re}(V_1 I_1^*) = \mathrm{Re}\left(V_1\left(\frac{n_1V_S - V_1}{jX_{t1}}\right)^*\right) \quad \cdots \quad (6)$$

$$P_2 = \mathrm{Re}(V_{pq} I_L^*) = \mathrm{Re}\left(V_{pq}\left(\frac{V_S + V_{pq} - V_R}{jX_{t2}}\right)^*\right) \quad (7)$$

d) The relationship between the inverter dc and the two transformers primary sides' voltages is obtained from pulse width modulation (PWM) control techniques from, N. Mohan, T. M. Undeland, and W. P. Robbins as:

$$V_1 = m_1V_{dc}/V_b \quad \cdots \quad (8)$$

$$V_2 = m_2V_{dc}/V_b \quad \cdots \quad (9)$$

$$V_{pq} = m_2V_{dc}/V_b/n_2 \quad \cdots \quad (10)$$

where;

m1 and m2 are the PWM indices, V1 and V2 are in p.u, Vb is the ac system base voltage, and n2 is the series transformer turn ration.

The PWM control is performed to regulate inverter ac side voltages, in which the phase angles of the voltages V1 and V2 are controlled by the firing angles φ1 and φ2 of the two converters, and are related to the phase angle of the supply voltage (Vs) as:

$$\theta_1 = \theta_S - \phi_1 \quad \cdots \quad (11)$$

$$\theta_2 = \theta_S - \phi_2 \quad \cdots \quad (12)$$

$$\theta_{pq} = \theta_S - \phi_2 \quad \cdots \quad (13)$$

The desired modulation indices m1 & m2, and the firing angles φ1 and φ2 serve as outputs from the UPFC. Thus, the UPFC dynamics can be analyzed from Eqs. 11 – 13, and the variables m1, m2, φ1 and φ2 can be manipulated in order to inject voltage Vpq in series with the line and control the power flow along the transmission line.

The dc voltage control is achieved by manipulating the firing angle φ1 of VSC1, while the UPFC bus voltage control is achieved by controlling m1 of the PWM controller of VSC1.

The UPFC compensation voltage Vpq can be decomposed

as Vp and Vq shown in the phasors of Fig. 2.
Where Vp is perpendicular to Vs, and has much effect on the active power flow; and Vq is in phase with Vs and has impact on reactive power flow, C. M. Shen, F. Felix, S. Chen, and B. Zhang.

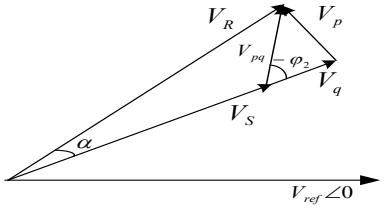

Figure 2: Transmission line voltage phasor with UPFC

3. METHODOLOGY

This section describes the methods used in achieving the objectives of the paper. To determine optimal location of the UPFC for damping inter-area mode oscillation in the power network, the following steps were carried out:

- ✓ Use the state space model of the system to perform modal analysis in order to identify the inter-area oscillatory mode of the system.
- ✓ Place the UPFC at various locations (buses and lines) of the network and compute the modal residue corresponding to the inter-area mode of the system.
- ✓ Identify the location that produces the largest residue index as the optimal location to place the UPFC.

In order to select the feedback signals for the systems control, then the following steps were observed.

- Place the UPFC at the identified optimal location on the network.
- Identify the various possible signals that could be used as feedback signals.
- Form the various models of the system with the identified feedback signals.
- Compute the open-loop zeros for each of the above system's model.
- Discard all models that produce positive (Right Half Plane) zeros.
- Compute Henkel Singular Values for the remaining models.
- Selected the model with the largest Henkel Norm.
- Compute RGA for the selected model.
- Identify the different possible control configurations for the system based on the above RGA.
- Test each configuration by closing the different loops and computing the PRGA for the sub-systems.
- Discard any configuration that produces negative relative gain after computing the PRGA.
- Select the configuration that does not have any negative gain as it satisfy the condition for ICI.
- Match the input-output signals according to the selected configuration.

3.1. Control Loop Interactions

This sub-section discusses analyses of the interactions involved in the design.

3.1.1. Relative Gain Array

A decentralised multivariable structure is ladened with interactions between different control loops Arzehu, N. A. et al., (2018). It is therefore pertinent to carefully select a pair of input-output variables that produce the least interactions with the rest of the control loops. Often, the RGA is the tool applied in analyzing such interactions for selecting the optimum control loops. The RGA is a matrix of which elements are indices obtained from the

relative gains of the system, defined as the ratio between open-loop gains to closed-loop (y_i/u_j: y_i/u_j), V. M. Jovica, and A. C. Serrano (2004) and C. Li-Jun, E. István (2006).

The steady-state model of a multivariable system can be represented by the following equations;

$$y_1 = k_{11}u_1 + k_{12}u_2 + ...k_{1n}u_n \quad \cdots \quad (14)$$

$$y_2 = k_{21}u_1 + k_{22}u_2 + ...k_{2n}u_n \quad \cdots \quad (15)$$

$$y_n = k_{n1}u_1 + k_{n2}u_2 + ...k_{nn}u_n \quad \cdots \quad (16)$$

This can be represented by the matrix equation;

$$y = \begin{bmatrix} y_1 \\ \vdots \\ y_n \end{bmatrix} \quad \cdots \quad (17)$$

$$u = \begin{bmatrix} u_1 \\ \vdots \\ u_n \end{bmatrix} \quad \cdots \quad (18)$$

$$G = \begin{bmatrix} G_{11} & \cdots & G_{1n} \\ \vdots & \ddots & \vdots \\ G_{n1} & \cdots & G_{nn} \end{bmatrix} \quad \cdots \quad (19)$$

$$y(s) = G(s)u(s) \quad \cdots \quad (20)$$

where,

G(s) is the transfer function matrix for the system. u(s) and y(s) are vectors of the input and output variables.

3.1.2. Open-Loop Gains

The open-loop gain is the gain between the input u_j and the output y_i when all outputs are not controlled, that is when the rest of the loops are open and other input changes are zero as shown in Fig. 3.

$$\left.\frac{\partial y_i}{\partial u_j}\right|_{u_k cons\tan t, k\neq j} = k_{ij} \quad \cdots \quad (21)$$

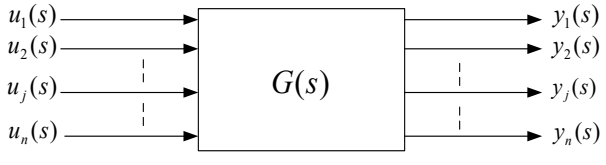

Figure 3: Open-loop gains, G. Rogers (2008)

3.1.3. Close-Loop Gains

The closed-loop gain is the gain between the input u_j and the output y_i when the rest of the outputs are under perfect control, that is when the rest of the loops are closed and other output changes are zero as depicted in Fig. 4.

$$\left.\frac{\partial y_i}{\partial u_j}\right|_{y_k cons\tan t, k\neq i} = k_{ij} \quad \cdots \quad (22)$$

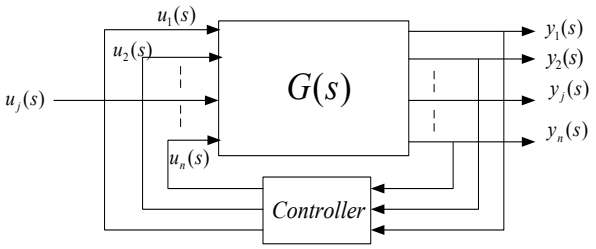

Figure 4: Closed-loop gains, G. Rogers (2008)

The relative gain array is thus;

$$\lambda_{ij} = \frac{\left.\frac{\partial y_i}{\partial u_j}\right|_{u_k\ constant, k\neq j}}{\left.\frac{\partial y_i}{\partial u_j}\right|_{y_k constant, k\neq i}} = \frac{Gains\ with\ open\ loops}{Gains\ with\ closed\ loops} \quad \cdots \quad (23)$$

From Eqn (23) it can be deduced that RGA is a matrix of relative gains that describes complete steady-state behavioral interaction of the system. However, RGA can also directly be from gain matrix G(s) in terms of Hadamard product in element-wise matrix multiplication as follows, S. Skogestad and I. Postlethwaite (2005); G. Rogers (2008):

$$\Lambda(G) = GoG^{-T} \quad \cdots \quad (24)$$

Relative Gain Array

$$\Lambda(G) = GoH = \begin{bmatrix} \lambda_{11} & \cdots & \lambda_{1n} \\ \vdots & \ddots & \vdots \\ \lambda_{n1} & \cdots & \lambda_{nn} \end{bmatrix} \quad \cdots \quad (25)$$

Where

$$H = \left(G^{-1}\right)^T = \begin{bmatrix} H_{11} & \cdots & H_{1n} \\ \vdots & \ddots & \vdots \\ H_{n1} & \cdots & H_{nn} \end{bmatrix} \quad \cdots \quad (26)$$

And

$$\lambda_{ij} = G_{ij} H_{ij} \quad \cdots \quad (27)$$

The relative gain λ_{ij} is hence a measure of the effect of other control loops in the system on the gain between u_j and y_i. The following rules were established to interpret the results of a given RGA, C. Li-Jun, E. István (2006):

1) $\lambda_{ij} = 1$, implies that there is perfect correlation between the controlled and the uncontrolled gains.
2) $\lambda_{ij} = 0$, implies that the input. u_j does not influence the output y_i.
3) $0 < \lambda_{ij} < 1$, implies that the gain is increased by the interactions of other control loops.
4) $1 < \lambda_{ij} < 10$, implies thatthe gain is reduced by the interactions of other control loops.
5) $\lambda_{ij} >> 10$, this implies that input-output pairing will make the system sensitive to small variations in gain.
6) $\lambda_{ij} < 0$, implies that as the uncontrolled gain decreases with increase in controlled gain, and vice versa.

Based on the above rules, the next section considers matching input and output signals with the relative gain closed to unity for a large decentralised multiple-input multiple-output (MIMO) system using partial relative gain array method (PRGA).

3.2. Partial Relative Gain Array

The literature shows no guaranty for stabilising a large decentralised MIMO system when RGA is used in selecting the input-output pairs. This is because some of the control loops may not be visible to RGA due to lack of integral controllability with integrity (ICI) in the system. A system is considered ICI if its stability is not affected by commissioning or decommissioning individual controllers within. Solving this problem requires further screening of the control structures, which could be achieved by the PRGA technique.

To implement the PRGA method, the relative gain array of the full open-loop is first determined. The system is then partially closed in order to assess the partial relative gain array. This way, the RPGA can unravel the ambiguity of input-output pairing of systems larger than two-by-two (2x2) which cannot be achieved easily by traditional RGAs, and hence provides a means of checking the system's ICI through the following equations, K. E.Haggblom (1997).

Let the system gain matrix G(s) be divided as

$$G(s) = \begin{bmatrix} G_{11} & \vdots & G_{12} \\ \cdots & \vdots & \cdots \\ G_{21} & \vdots & G_{22} \end{bmatrix} \quad \cdots \quad (28)$$

The effective gain of the sub-system $G_{11}(s)$ when part of the system $G_{22}(s)$ is given as:

$$\overline{G}_{11} = G_{11} - G_{12} G_{22}^{-1} G_{21} \quad \cdots \quad (29)$$

Let $\bar{G}_m(s)$ represent the transfer matrix of subsystem $G_m(s)$ when the rest of the system is under feedback control, then PRGA for the sub-system $G_m(s)$ is given as:

$$\Lambda_m^p(G) = \Lambda(\overline{G}_m) = \overline{G}_m o \overline{G}_m^{-T} \quad \cdots \quad (30)$$

The matrix obtained from Equation (30) can then be used to further screen the system's control structure in order to check the system's integral controllability with integrity (ICI).

4. RESULTS AND DISCUSSION

Six possible scenarios were configured in Table 1, to study the matching of the input-output pairs that best satisfy oscillation damping in a UPFC controlled 2-area, 13-bus network, first using the traditional RGA. It was found out that only one configuration via VSC-2 produced the desired outcomes such that; the converter was able to control the reactive power flow from bus-3 to bus-101, as well as controlled the real power flow from

bus-11to bus-110. On the other hand, VSC-1 was also able to inject the required bus voltage in series to control reactive power from bus-11 to bus-110, while the UPFC (VSC1 & VSC2 hybrid) injected the desired common dc voltage component to control reactive power from bus-101 to bus-13 for ensuring systems Integral controllability with Integrity (ICI) as verified in the following case studies.

Table 1: Possible control configurations

Configurations	Pairings	Relative Gains
C4123	(y1, u4), (y2, u1), (y3, u2), (y4, u3)	3.8339, 0.0282, 0.0159, 1.0505
C4132	(y1, u4), (y2, u1), (y3, u3), (y4, u2)	3.8339, 0.0282, 0.0668, 0.2746
C4213	(y1, u4), (y2, u2), (y3, u1), (y4, u3)	3.8339, 0.0028, 0.1550, 1.0505
C4231	(y1, u4), (y2, u2), (y3, u3), (y4, u1)	3.8339, 0.0028, 0.0668, 2.2238
C4312	(y1, u4), (y2, u3), (y3, u1), (y4, u2)	3.8339, 0.0164, 0.1550, 0.2746
C4321	(y1, u4), (y2, u3), (y3, u2), (y4, u1)	3.8339, 0.0164, 0.0159, 2.2238

4.1 Case study

The model of the 2-area 4-machine power system with the UPFC as shown in Fig. 5 was developed from the network data obtained from,), V. M. Jovica, and A. C. Serrano (2004) and C. Li-Jun, E. István (2006).

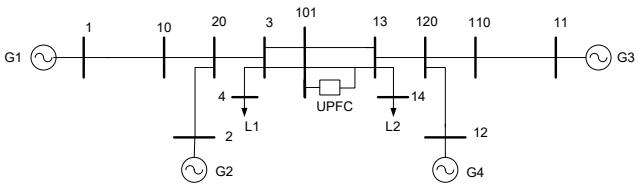

Figure 5: Two-area network with UPFC

The performance of the system was simulated in MATLAB environment with the following variables as output signals:

- Y1- current from bus-3 to bus-101.
- Y2- real power from bus-11to bus-110.
- Y3- reactive power from bus-11 to bus-110.
- Y4- reactive power from bus-101 to bus-13.

And the following variables as the reference Input signals:

- U1- VSC-1 bus voltage.
- U2- UPFC common dc voltage.
- U3- VSC-2 injected real power.
- U4- VSC-2 injected reactive power.

The steady state gain matrix G(s) for the system is obtained as:

$$G(s)=\begin{bmatrix} -1.6263 & -0.0007 & 0.7114 & -0.3496 \\ -0.8719 & -0.0004 & 0.4430 & -0.1969 \\ -35.0168 & -0.0137 & 14.0588 & -7.2928 \\ -1.6304 & -0.0007 & 0.7157 & -0.3510 \end{bmatrix} \cdots (31)$$

The Relative Gain Array for the system is:

$$\Lambda(Gs)=e^{4}x\begin{bmatrix} -0.4070 & -0.2932 & -1.1336 & 3.8339 \\ 0.0282 & 0.0028 & 0.0164 & -0.0474 \\ 0.1550 & 0.0159 & 0.0668 & -0.2377 \\ 2.2238 & 0.2746 & 1.0505 & -3.5487 \end{bmatrix} \cdots (32)$$

Different possible control configurations for the system based on the above RGA is given in Table 1. The table was used to conduct the following tests.

TEST No. 1: Configuration C4123 and C4132, while loop – (y2, y1) is closed under feedback control. The transfer matrix of subsystem $G_m(s)$ then becomes:

$$\overline{G}_{2034}=\begin{bmatrix} \cdots & 0.0000 & -0.1149 & 0.0177 \\ *** & \cdots & \cdots & \cdots \\ \cdots & 0.0024 & -3.7327 & 0.6150 \\ \cdots & 0.0000 & -0.1127 & 0.0172 \end{bmatrix} \cdots (33)$$

Hence, the PRGA for the sub-system G_m s) also becomes

$$\Lambda(\overline{G}_{2034})=e^{3}x\begin{bmatrix} \cdots & 0.1144 & 1.8306 & -1.9441 \\ *** & \cdots & \cdots & \cdots \\ \cdots & -0.0223 & -0.1773 & 0.2007 \\ \cdots & -0.0911 & -1.6523 & 1.7444 \end{bmatrix} \cdots (34)$$

Based on the above PRGA the possible control configuration C4123 and 4132 do not satisfy the condition for ICI (Integral Controllability with Integrity) because of the presence of negative signs in the arrays.

TEST No. 2: Configuration C4213 and C4231, loop – (y2, u2) is closed under feedback control. The transfer matrix of subsystem $G_m(s)$ then becomes

$$\overline{G}_{1034} = \begin{bmatrix} -0.1005 & \cdots & -0.0638 & -0.0050 \\ \cdots & *** & \cdots & \cdots \\ -5.1542 & \cdots & -1.1140 & -0.5490 \\ -0.1046 & \cdots & -0.0595 & -0.0064 \end{bmatrix} \cdots (35)$$

Hence, the PRGAfor the sub-system $G_m(s)$ also becomes

$$\Lambda(\overline{G}_{1034}) = e^3 x \begin{bmatrix} -0.9040 & \cdots & 1.3361 & -0.4311 \\ \cdots & *** & \cdots & \cdots \\ 0.1910 & \cdots & -0.0731 & -0.1169 \\ 0.7140 & \cdots & -1.2620 & 0.5490 \end{bmatrix} \cdots (36)$$

Based on the above PRGA, configuration C4213 andC4231 also do not satisfy the conditions for ICI.

TEST No. 3: Configuration C4312 and C4321, loop - (y2, u3) is closed under feedback control. The transfer matrix of the subsystem Gm(s) becomes:

$$\overline{G}_{1204} = \begin{bmatrix} -0.2261 & -0.0001 & \cdots & -0.0334 \\ \cdots & \cdots & *** & \cdots \\ -7.3467 & -0.0010 & \cdots & -1.0441 \\ -0.2218 & -0.0001 & \cdots & -0.0329 \end{bmatrix} \cdots (37)$$

Hence, the PRGA for the sub-system $G_m(s)$ then becomes

$$\Lambda(\overline{G}_{1204}) = e^3 x \begin{bmatrix} -3.3466 & -0.3092 & \cdots & 3.6567 \\ \cdots & \cdots & *** & \cdots \\ 0.3251 & 0.0157 & \cdots & -0.3398 \\ 3.0224 & 0.2945 & \cdots & -3.3159 \end{bmatrix} \cdots (38)$$

Based on the above PRGA configurations, C4312 and C4321 seem to satisfy the conditions for ICI, so further investigation is required. Therefore, loop – (y1, u4) is closed under feedback control. The transfer matrix of the sub-system $G_m(s)$ is given as

$$\overline{G}_{0123} = \begin{bmatrix} \cdots & \cdots & \cdots & *** \\ 0.0441 & -0.0000 & 0.0423 & \cdots \\ -1.0915 & 0.0009 & -0.7813 & \cdots \\ 0.0024 & 0.0000 & 0.0015 & \cdots \end{bmatrix} \cdots (39)$$

Hence, the PRGA for the sub-system Gm(s) is computed as

$$\Lambda(\overline{G}_{0123}) = \begin{bmatrix} \cdots & \cdots & \cdots & *** \\ -14.3155 & -0.3199 & 15.6354 & \cdots \\ 48.2281 & -10.1055 & -37.1226 & \cdots \\ -32.9126 & 11.4255 & 22.4872 & \cdots \end{bmatrix} \cdots (40)$$

Based on the above PRGA, configuration C4132 does not satisfy the condition for ICI, while configuration C4312 does. Therefore, the best signal matching can be deduced as:

Y1 – U4: That is the current flow from bus-3 to bus-101 against VSC-2, injected reactive power (Q).

Y2 – U3: That is real power flow from bus-11to bus-110 against VSC-2, injected real power (P).

Y3 – U1: That is reactive power flow from bus-11 to bus-110 against VSC-1, provided bus voltage support.

Y4– U2: That is reactive power flow from bus-101 to bus-13 against UPFC, provides common dc voltage support.

The impact of the UPFC on the system can further be observed from Figures 6 – 10, which depict the responses of the terminal voltages and active power at generator buses to step changes in the generators excitation reference voltages. The systems with UPFC are presented as “blue dotted-lines”, and the ones without UPFC are represented as “red dotted-lines”, respectively.

It can be seen that in all the cases, the UPFC has eliminated the steady state error in the system’s response and has reduced the settling time to less than 4 seconds.

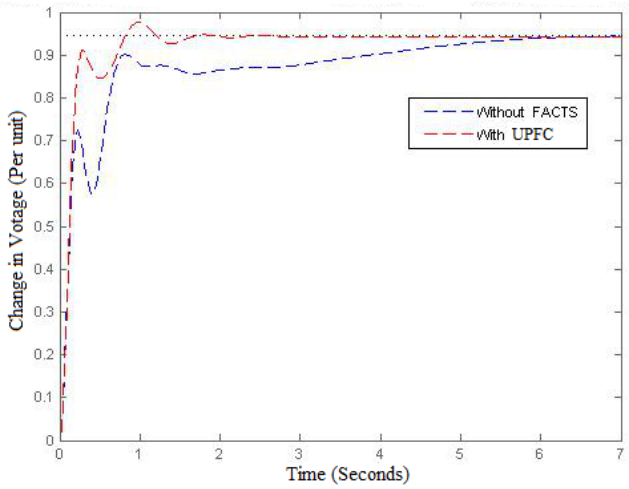

Figure 6: Step voltage response at bus-1 to Gen-1

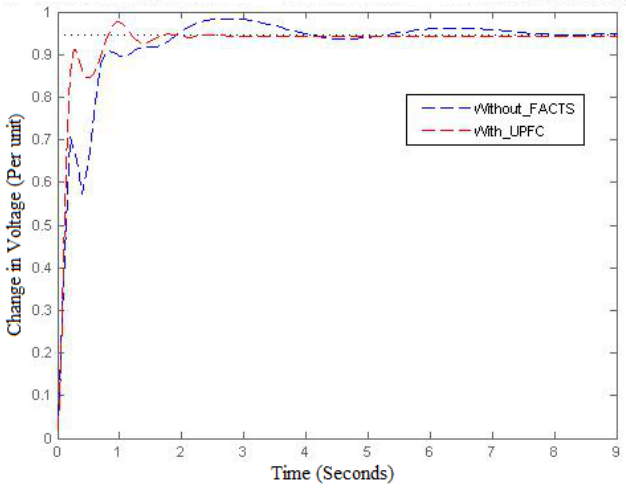

Figure 7: Step voltage response at bus-2 to Gen-2

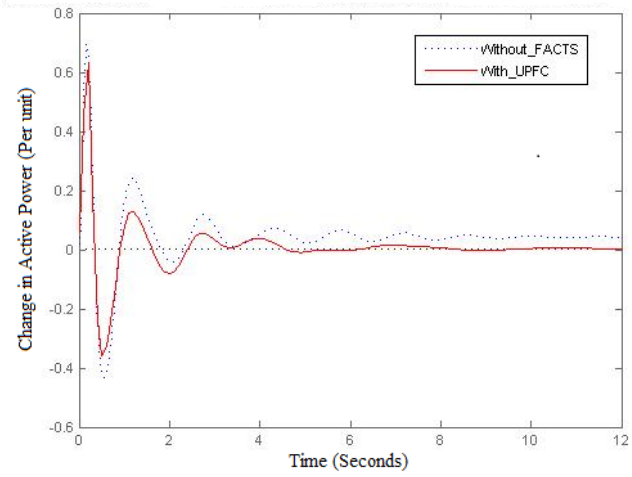

Figure 8: Active power response at bus-3 to Gen-3

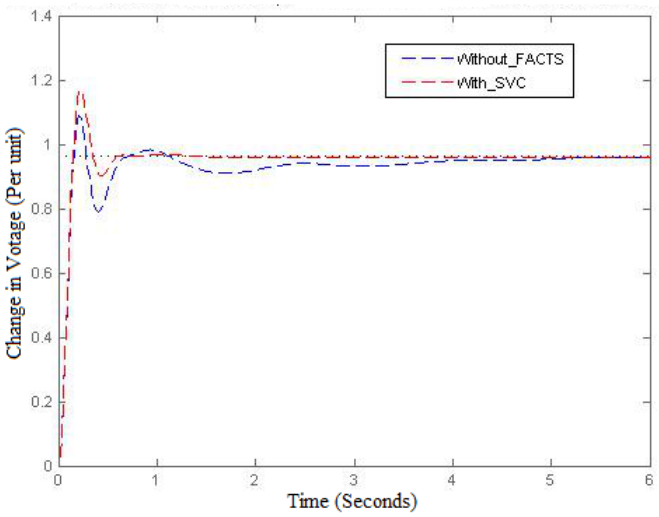

Figure 9: Step voltage response at bus-3 to Gen-3

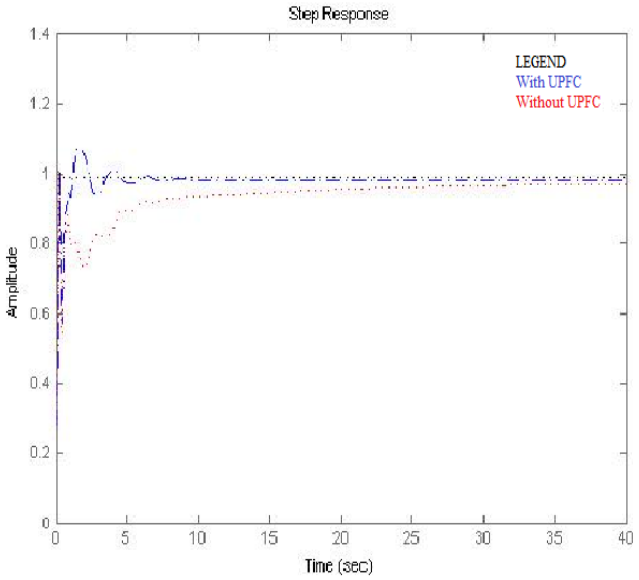

Figure 10: Step voltage response at bus-4 to Gen-4

5. CONCLUSION

This paper has used partial relative gain array (PRGA) technique to select and match the optimum control signals in a configured UPFC to appropriately damp inter-area oscillations. A 2-area 4-machine power system was used to demonstrate that the technique could select the signals that satisfy the necessary conditions in what is referred to in power stability analysis as the system's "integral controllability with integrity (ICI)" index. This failure tolerance phenomenon is often very difficult to achieve using the conventional relative gain array (RGA) method as validated in this study.

Consequently, 2-area 13-bus system is used to implement this technique, and it has proven to be more effective in determining the integral controllability with integrity (ICI) of uncertain modelling errors with increased sensitivity as compared to the traditional GRA technique. This is confirmed under test case number 3 which was based on the PRGA configurations C4312 and C432, and given by Equation 39. Using PRGA technique, appropriate control signals were selected that were used to shift the critical eigenvalues of the power system more to the left of j-ω axis, thereby damping the inter-area oscillations by increasing the damping ratio from 0.0231 to 0.13, and reducing the damping rate from 6 seconds achieved without UPFC down to 4 seconds with UPFC.

6. REFERENCES

Taylor C. W. (1994) *Power System Voltage Stability*, McGraw-Hill.

Bikash P. and Balarko C. (2005), Robust Control In Power Systems. Springer Science + Business Media, Inc , 233 Spring Street, New York, NY10013 USA, ISBN 0-387-25949-X.

Magaji N. and Mustafa M. W. (2008), Optimal Location of FACTS devices for damping oscillations. 2nd IEEE International Conference on Power and Energy (PECon 08),

Kazemi A. and Andami H, (2004), FACTS Devices in Deregulated Electric Power Systems: Review IEEE International Conference on Electric Utility Deregulation, Restructuring and Power Technologies, Hong Kong, pp. 337- 342.

Zhang P, et al (1998). Selection of locations and input signals for multiple SVC damping controllers in large scale power systems. In Proc. IEEE Power Eng. Soc. Winter Meeting, Paper IEEE-0-7803-4403-0, pp. 667–670.

Magaji N. and Mustafa M. W, (2009). Optimal Location and Signal Selection of SVC Device for Damping Oscillation. International Review on Modelling and Simulations vol. 2, pp. 144-151.

Farsangi M. M.. et al (2004). Choice of FACTS device control input for damping inter-area oscillations. IEEE Trans.Power System, vol. 19, pp. 1135–114.

Skogestad S. and Postlethwaite I., (2005). Multivariable Feedback Control: Analysis andDesign (2nd Edition). UK: Wiley.

Chen D. Z. et al (2006). Interaction assessment of FACTS control by RGA for the effective design of FACTS damping controllers. IEE Proceeding in Generation, Transmission and Distributions, vol. 153, pp. 610-616.

Nabavi Niaki S. A, and Reza Iravani M., (2002). Application of Unified Power Flow Controller for Damping Inter area Oscillation. IEEE Conference 0-7803-7525-4/02 pp. 348-353. Z. Huang, N. Yixin,

Shen C. M. et al (2000). Application of Unified Power

Flow Controller in Interconnected Power Systems-Modeling, Interface, Control Strategy, and Case Study. IEEE Transactions On Power Systems, Vol. 15 No. 2.

Saxena R. D. et al (2012). Application of Unified Power Flow Controller (UPFC) for Damping Power System Oscillations. – A Review International Journal of Engineering Research & Technology (IJERT)Vol. 1 Issue 4. College of Engineering, Nagpur (India).

Rogers G., (2008). Linearized Analysis of Power System Dynamics with MatNetEig**.** Graham RogersRR#5 Colborne, Ontario K0K 1S0 Canada cherry@eagle.ca.

Mohan N.et al (1995). Power Electronics: Converters, Applications and Design, Second Edition: John Wiley & Sons.

Jovica V. M., and Serrano A. C., (2004). Identification of Electromechanical Modes and Placement of PSSs Using Relative Gain Array. IEEE Trans. Power Systems, vol. 19, pp. 410-417.

Li-Jun C., István E., (2006). Identification of the Interactions among the Power System Dynamic Voltage Stability Controllers using Relative Gain Array. University Teknologi Malaysia. 142440178X.

Haggblom K. E., (1997). Partial Relative gain Array: A new Tool for Control Structure Selection. Faculty of Chemical Engineering, Abo Akademi University, Finland. AIChE Annual meeting paper 193h. Los Angeles, USA.

Kundur P., (2004) Power system stability and control. New York USA: McGraw- Hill.

Alok P S, and Sonam S., (2013) Critical Review on Power Oscillation Damping Controllers. International Journal of Science and Research (IJSR) ISSN (Online): 2319-7064.

José L-G et al., (2014). Input–output signal selection for damping of power system oscillations using wind power plants. International Journal of Electrical Power & Energy Systems. Volume 58, Pages 75-84.

Dhanraj Chitara, et al., (2015). Optimal Tuning of Multimachine Power System Stabilizer using Cuckoo Search Algorithm. Available online at www.sciencedirect.com, IFAC (International Federation of Automatic Control).

Arzehu, N. A. et al, (2018). Damping Low Frequency Oscillations via FACT-POD Controllers Tuned by Bees Algorithm. Journal of Electrical Engineering, Universiti Teknologi Malaysia, vol. 17, pp. 6-14.

Jeffrey Uhlmann (2019). On the Relative Gain Array (RGA) with Singular and Rectangular Matrices, University of Missouri-Columbia 201 Naka Hall, Columbia, MO 65211 573.884.2129.